

Dirac Spectrum, Axial Anomaly and the QCD Chiral Phase Transition *

Shailesh Chandrasekharan and Norman Christ

Department of Physics, Columbia University,
New York, NY 10027, USA

The QCD phase transition is studied on 16^3 and $32^3 \times 4$ lattices both with and without quark loops. We introduce a new zero-flavor or quenched species of quark ζ and study the resulting chiral condensate, $\langle \bar{\zeta}\zeta \rangle$ as a function of the ζ mass, m_ζ . By examining $\langle \bar{\zeta}\zeta \rangle$ for $10^{-10} \leq m_\zeta \leq 10$ we gain considerable information about the spectrum of Dirac eigenvalues. A comparison of $ma = 0.01$ and 0.025 shows little dependence of the Dirac spectrum on such a light, dynamical quark mass, after an overall shift in β is removed. The presence of sufficient small eigenvalues to support anomalous chiral symmetry breaking in the high temperature phase is examined quantitatively. In an effort to enhance these small eigenvalues, $\langle \bar{\zeta}\zeta \rangle$ is also examined in the pure gauge theory in the region of the deconfinement transition with unexpected results. Above the critical temperature, the three Z_3 phases show dramatically different chiral behavior. Surprisingly, the real phase shows chiral symmetry, suggesting that a system with one flavor of staggered fermion at $N_t = 4$ will possess a chiral a phase transition—behavior not expected in the continuum limit.

1. INTRODUCTION

The spectrum of the Dirac operator is closely related to a number of important aspects of finite temperature QCD. First, a non-zero density of small eigenvalues is necessary for spontaneous chiral symmetry breaking[1]. Second, if the QCD phase transition is second order, one expects this eigenvalue spectrum to show critical behavior for $T \approx T_c$. Third, the Dirac spectrum should be particularly sensitive to the effects of quark loops since the Dirac determinant for small quark mass strongly suppresses gauge configurations with small Dirac eigenvalues. Finally, the universality arguments which predict the order of the QCD phase transition[2], rely on the explicit breaking of the continuum $U_A(1)$ symmetry by the axial anomaly. Such anomalous symmetry breaking requires a significant density of small eigenvalues.

Since it is difficult to obtain the information about the spectrum directly we choose to examine a less familiar quantity: the quenched or zero-flavor chiral condensate for an auxiliary quark

field $\zeta(x)$ with mass m_ζ . By studying the dependence on m_ζ , we obtain interesting, qualitative information about the spectrum, which suggests unexpected behavior near the QCD phase transition.

We begin with a normal, full QCD simulation at finite temperature described by the partition function:

$$Z_{m,\beta} = \Pi_l \int d[U_l] e^{-\beta S_g} \det(D + m)^{N_f/4}. \quad (1)$$

Here the integral is performed over all link matrices U_l and the gauge action S_g is given by

$$S_g = -\frac{1}{3} \sum_{\mathcal{P}} \text{re tr } U_{\mathcal{P}} \quad (2)$$

with $U_{\mathcal{P}}$ the ordered product of the four matrices associated with the fundamental plaquette \mathcal{P} . We use the staggered fermion Dirac operator D .

The determinant entering the partition function in Eq. 1 represents the effects of quark loops, for N_f flavors of quarks of mass m . We will refer to the corresponding lattice quark fields as $\chi(x)$. In this paper we introduce a second species of fermions, $\zeta(x)$, with mass m_ζ which will appear in observables but does not enter the quark determinant. These ζ fermions may be thought of

*This work was done in collaboration with Dong Chen, Weonjong Lee, Robert Mawhinney, and Decai Zhu. The work was supported in part by the US department of Energy.

as quenched or $N_f = 0$ quarks. We then compute the expectation value of the quantity $\bar{\zeta}\zeta$ in the thermal background specified by the partition function of Eq. 1. Thus,

$$\langle \bar{\zeta}\zeta(x) \rangle = \left\langle \left\langle x \left| \frac{1}{(D + m_\zeta)} \right| x \right\rangle \right\rangle_{\beta, m} \quad (3)$$

where the average $\langle \rangle_{\beta, m}$ is calculated using the distribution of gauge fields in the QCD path integral. Although this quantity is no easier to compute than the normal chiral condensate $\langle \bar{\chi}\chi \rangle$, the mass m_ζ can be varied without changing the mass m which enters the Boltzmann factor and which must be fixed during a particular Monte Carlo run. Typically we study 25 values of m_ζ .

This quantity is of special interest because it is a simple transform of the Dirac eigenvalue density. If we evaluate the propagator in Eq. 3 by inserting a complete set of eigenfunctions of D , and averaging over x , we find

$$\langle \bar{\zeta}\zeta \rangle(m_\zeta) = 2m_\zeta \int_0^\infty \frac{\rho(\lambda)}{(\lambda^2 + m_\zeta^2)} d\lambda. \quad (4)$$

Here we have exploited the γ^5 symmetry which makes the Dirac spectrum symmetric about zero and introduced $\rho(\lambda)$, the Dirac eigenvalue density per unit volume, averaged over the thermal distribution of Eq. 1. The function $\rho(\lambda)$ depends on β and the dynamical quark mass m .

Thus, $\langle \bar{\zeta}\zeta \rangle$ is a transform of the Dirac spectrum, strongly weighted toward eigenvalues $\lambda \sim m_\zeta$. Note the $U(1)$ chiral symmetry for the quark field ζ , present in the staggered fermion formulation, implies that $\langle \bar{\zeta}\zeta \rangle$ should vanish as $m_\zeta \rightarrow 0$. Spontaneous breaking of this symmetry results if $\rho(0) \neq 0$. In which case the explicit factor of m_ζ in the numerator of Eq. 4 is compensated by the linear divergence of the λ integral as $m_\zeta \rightarrow 0$. The result is the Banks-Casher formula[1]:

$$\langle \bar{\zeta}\zeta \rangle(m_\zeta = 0) = \pi\rho(0). \quad (5)$$

Thus, we argue that the function $\langle \bar{\zeta}\zeta \rangle(m_\zeta)$ is easy to compute, contains information about the spectrum of Dirac eigenvalues and is closely connected to spontaneous symmetry breaking. In fact, as we discuss below, the infrared behavior of $\langle \bar{\zeta}\zeta \rangle(m_\zeta \rightarrow 0)$ also determines the character of

anomalous chiral symmetry breaking, a quantity difficult to study directly with lattice fermions.

2. $N_f = 2$ CHIRAL TRANSITION

2.1. Critical Behavior

Figure 1 shows the quantity $\langle \bar{\zeta}\zeta \rangle$ as a function of m_ζ for a series of values of β in the critical region. These results were obtained on a $16^3 \times 4$ lattice with two degenerate flavors of dynamical fermions of mass $ma = 0.01$. Note, this is a log-log plot showing six orders of magnitude variation in m_ζ . As can be seen, the behavior is quite complex.

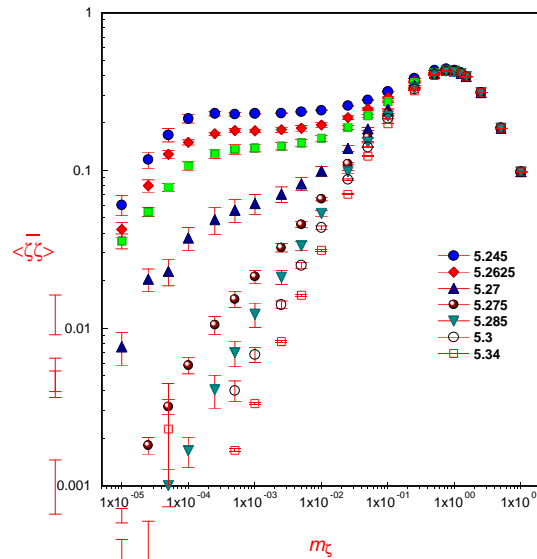


Figure 1. The expectation value $\langle \bar{\zeta}\zeta \rangle$ plotted as a function of the mass m_ζ for a series of values of β . Shown are two-flavor calculations with quark mass $ma = 0.01$ on a $16^3 \times 4$ volume.

First consider β in the low temperature, chirally asymmetric region, $\beta \leq \beta_c$. For $m_\zeta \geq 10^{-2}$, $\langle \bar{\zeta}\zeta \rangle$ shows a complex non-linear behavior much of which is certainly due to finite lattice spacing effects. (In the continuum limit a simple linear behavior is expected for large m_ζ with a quadratically divergent coefficient.) For $10^{-4} \leq m_\zeta \leq 10^{-2}$ a constant plus linear fit

works well, at least for those values of β farthest from β_c . For $m_\zeta \leq 10^{-4}$ finite volume effects set in and $\langle \bar{\zeta}\zeta \rangle$ approaches zero linearly as expected. It is interesting to note that a somewhat more elaborate fit, writing $\langle \bar{\zeta}\zeta \rangle$ as the sum of a constant and fractional power, $\langle \bar{\zeta}\zeta \rangle = c_0 + c_1 m_\zeta^y$ works well over a significantly larger mass range $10^{-4} \leq m_\zeta \leq 0.05$ using a single value of $y \approx 0.6$. Such a fit merges nicely with a description which holds at $\beta = \beta_c \approx 5.275$, where only a fractional power, close to 0.6, is seen. Figure 2 shows our $\beta = 5.245, 5.2625$ and 5.265 data together with these constant plus linear and constant plus fractional power fits. For the smallest value, $\beta = 5.245$, the simple constant plus linear fit works nicely. However, for the more nearly critical $\beta = 5.265$, Figure 2 shows the constant plus fractional power working visibly better.

For $\beta \geq 5.275$, a fractional power, $\langle \bar{\zeta}\zeta \rangle = c m_\zeta^y$, begins to fit well with the power growing with increasing β so that by $\beta = 5.34$ the power is $y = 0.98$, very close to 1.0, the expected linear dependence on m_ζ at high temperature. Figure 3 shows these fits for $\beta = 5.27, 5.275, 5.285$ and 5.34 . For the smallest β value, 5.27, a pure fractional power does not fit well—a constant term is also needed while for the larger values of β a pure fractional power, with zero intercept, works quite well. At these larger values of β the fits work at even lower masses suggesting that the region of small eigenvalues, $\lambda \leq \approx 10^{-4}$, which may be distorted by finite volume effects, is less important.

If we attempt to study the critical behavior of $\langle \bar{\chi}\chi \rangle$ as a function of the quark mass m , there are many predictions of universality[3]. For example, at T_c , one expects $\langle \bar{\chi}\chi \rangle = \kappa_1 m^{1/\delta}$ for $m \rightarrow 0$. Of course, this singular behavior in the mass can arise from a combination of the dependence of $\langle \bar{\chi}\chi \rangle$ on the quark mass as it enters both the propagator and fermion determinant. This dual role played by the quark mass can be seen explicitly by relating $\langle \bar{\chi}\chi \rangle$ and $\langle \bar{\zeta}\zeta \rangle$:

$$\langle \bar{\chi}\chi \rangle|_{\beta,m} = \langle \bar{\zeta}\zeta \rangle(m_\zeta = m)|_{\beta,m} \quad (6)$$

Here the mass in the quark propagator explicitly entering the expectation value, m_ζ , is often referred to as the valence mass, m_{val} , while the mass in the fermion determinant, m , used when

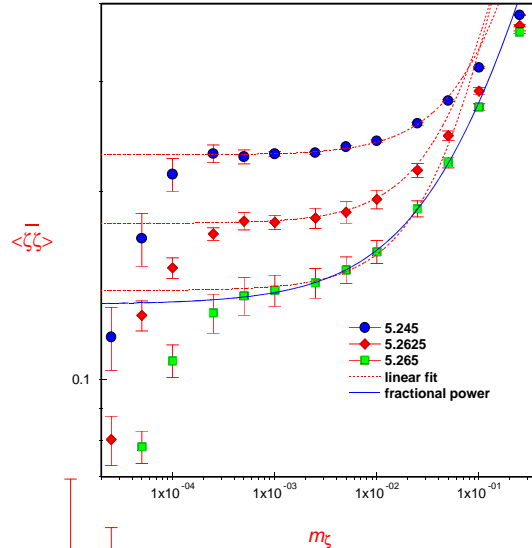


Figure 2. An expanded version of the previous $N_f = 2$ plot showing possible fits for $\beta \leq \beta_c$. These β values all show a non-zero intercept as $m_\zeta \rightarrow 0$, when extrapolated from the region $m_\zeta \geq 5 \times 10^{-4}$, a region apparently unaffected by finite volume distortions. Note how the constant plus fractional power fit agrees with the simulation over nearly three orders of magnitude for $\beta = 5.265$.

computing $\langle \bar{\zeta}\zeta \rangle$ is the sea quark mass, m_{sea} .

Thus, it is the dependence on m_{val} that we are investigating when we examine $\langle \bar{\zeta}\zeta \rangle$ as a function of m_ζ . Only if the simulations do not depend in a critical way on the quark mass in the determinant, should we attempt to compare our exponent $y|_{\beta=\beta_c}$ with $1/\delta$.

2.2. The High Temperature Phase

The fact that $\langle \bar{\zeta}\zeta \rangle$ appears to vanish with vanishing m_ζ when $\beta \geq \beta_c$ is a bit surprising. The conventional picture assumes the presence of topological configurations that break the $U_A(1)$ symmetry anomalously. This requires a significant density of small eigenvalues in the Dirac

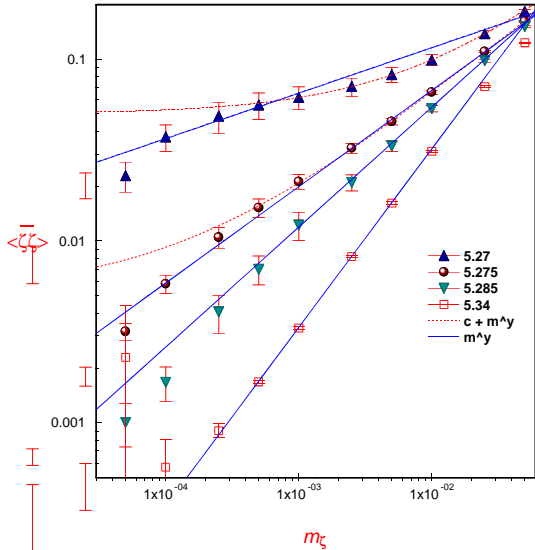


Figure 3. An expanded version of the previous $N_f = 2$ plot showing possible fits for $\beta \geq \beta_c$. These β values, except perhaps for $\beta = 5.27$, all show a zero intercept as $m_\zeta \rightarrow 0$, when extrapolated from the region $m_\zeta \geq 5 \times 10^{-4}$. Although a pure fractional power does not fit very well at the smallest β value shown, 5.27, for larger β this simple description works very well.

spectrum. For example, a dilute instanton gas, expected by some to describe the region above the critical point, would give a non-zero density of eigenvalues, $\rho(0) \neq 0$. Recall, that it is only for the physical quantity $\langle \bar{\chi}\chi \rangle$ that one expects the restoration of chiral symmetry. In the limit $m \rightarrow 0$ not only is the valence mass in the propagator, m_{val} vanishing, but also the mass in the determinant, m_{sea} is going to zero. It is the added suppression of small eigenvalues, coming from the zero quark mass limit of the fermion determinant, that is presumably required for chiral symmetry restoration above T_c .

Thus, a small sea quark mass should suppress the small eigenvalues associated with anomalous breaking of $U_A(1)$ symmetry in the high temperature phase. Since in this calculation we do not set m_{sea} to zero, one might expect that anomalous breaking of $U_A(1)$ symmetry will require $\langle \bar{\zeta}\zeta \rangle(m_\zeta \rightarrow 0) \neq 0$, contrary to what we see. Of course, this non-zero value of $\langle \bar{\zeta}\zeta \rangle$ will be sup-

pressed by factors of $m_{\text{sea}}a = 0.01$. For that reason we will examine larger dynamical quark masses and even a quenched calculation below.

2.3. Anomalous $U_A(1)$ Symmetry Breaking

Given the suppression of small eigenvalues that we see for $\beta > \beta_c$ it is natural to ask if we can see any evidence for anomalous symmetry breaking. This is an important question given the effects of such symmetry breaking on the order of the two-flavor phase transition.

Consider a continuum, two-flavor theory with $SU(2) \times SU(2)$ flavor symmetry (in the limit of vanishing fermion masses) above the phase transition. The axial anomaly is expected to break the anomalous $U_A(1)$, forcing the two-point functions constructed from the operators $\bar{\psi}\gamma^5\tau^i\psi$ and $\bar{\psi}\tau^i\psi$ to be unequal. (Here ψ is the continuum fermion field.) If these two-point functions are evaluated at zero momentum and subtracted, their anomalous $U_A(1)$ symmetry breaking difference (here called ω) can be written as follows:

$$\omega = 4m^2 \int_0^\infty \frac{\rho(\lambda)d\lambda}{(\lambda^2 + m^2)^2} \quad (7)$$

We can compare this equation with our results for the behavior of $\rho(\lambda)$ as $\lambda \rightarrow 0$ at fixed quark mass. In fact, the behavior of $\langle \bar{\zeta}\zeta \rangle$ as $m_\zeta \rightarrow 0$ for β just above β_c suggests that $\rho(\lambda) \sim c(m)\lambda^y$ for $0 < y < 1$ which would suggest $\omega \sim c(m)m^{(y-1)}$. However, the fermion determinant may well suppress the small eigenvalues, with $c(m)$ vanishing as m goes to zero.

We can relate ω directly to our quantity $\langle \bar{\zeta}\zeta \rangle(m_\zeta)$:

$$\omega = \frac{\langle \bar{\chi}\chi \rangle}{m} - \frac{\partial}{\partial m_\zeta} \langle \bar{\zeta}\zeta \rangle|_{m_\zeta=m} \quad (8)$$

and attempt to study how it varies as $m \rightarrow 0$. Figure 4 shows the quantity ω for a series of values of $\beta > \beta_c$ at $ma = 0.01$ and at $\beta = 5.327$ for $ma = 0.025$. Clearly ω is non-zero in this region and does not appear to decrease as ma decreases from 0.025 to 0.01 provided we adjust β to remain a fixed displacement above β_c . Thus, this calculation appears to show the presence of anomalous symmetry breaking for $N_f = 2$, in the high temperature phase, just above the transition.

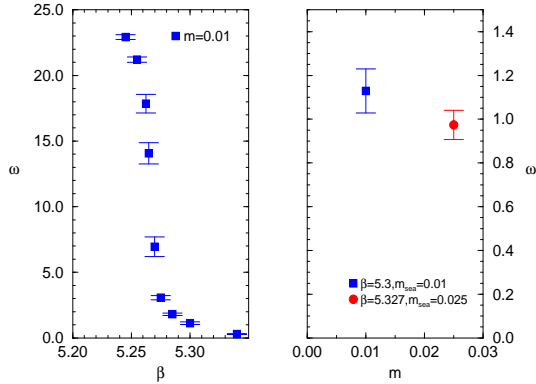


Figure 4. The quantity ω which directly measures the strength of anomalous symmetry breaking plotted versus β . On the left side results for $ma = 0.01$ are shown while on the right, results for $ma = 0.01$ and 0.025 are compared at $\beta = 5.3$ and 5.327 respectively.

3. EFFECTS OF QUARK LOOPS

In order to address the effects of the fermion determinant, let compare our $ma = 0.01$ and 0.025 results in greater detail. We find that even when comparing the quantity $\langle \bar{\zeta} \zeta \rangle$ evaluated over the entire range of m_ζ , the $ma = 0.01$ and $ma = 0.025$ simulations can be made to agree within a few percent if we allow for a quark-mass dependent shift in β . In Figure 5 we show $\langle \bar{\zeta} \zeta \rangle$ computed at $\beta = 5.272$, $ma = 0.025$ compared to a group of $ma = 0.01$ results. The quite precise 5-6% agreement with the $\beta = 5.255$, $ma = 0.01$ curve over the entire m_ζ range is striking. Similarly, for higher temperatures, Figure 6 shows $\langle \bar{\zeta} \zeta \rangle$ computed at $\beta = 5.327$, $ma = 0.025$ compared to $ma = 0.01$ results. Again, we see 5-6% agreement with the $\beta = 5.3$, $ma = 0.01$ curve over the entire m_ζ range. Thus, in both the chirally symmetric and asymmetric phases, the change in dynamical quark mass from 0.01 to 0.025 can be quite accurately compensated by a simple shift in β . No disparate effects on low or high eigenvalues are seen. The shift in β of 0.027 needed in the high temperature phase is precisely the shift in β_c that we identified earlier when comparing

β_c found in our 0.01 and 0.025 simulations.

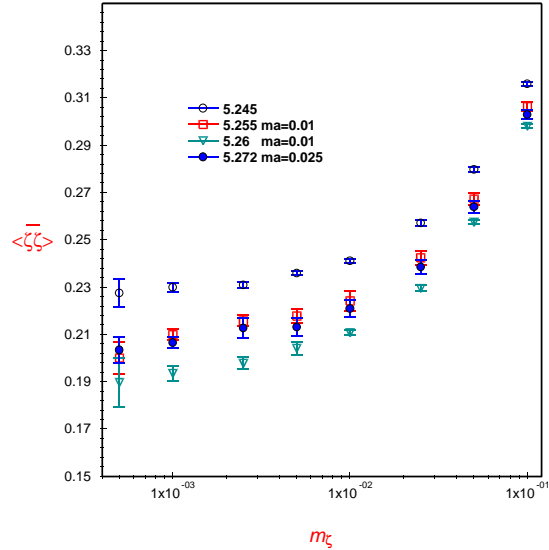


Figure 5. The quantity $\langle \bar{\zeta} \zeta \rangle$ plotted as a function of m_ζ for $\beta = 5.272$ and $ma = 0.025$. It is compared with $ma = 0.01$ results for three values of β . The close agreement with the $ma = 0.01$, $\beta = 5.255$ curve is evident.

It is interesting to note that the 0.017 shift in β found in the low temperature regime is substantially smaller than the 0.027 shift needed at high temperature. Thus, it is clearly incorrect to describe the effects of quark loops as causing a simple shift in β . At the least, that shift is itself β -dependent.

4. QUENCHED CHIRAL TRANSITION

As has been discussed above, we have not seen the effects of small eigenvalues for $\beta > \beta_c$ in our $ma = 0.01$, full QCD simulations to the extent expected, for example, from a model of dilute instantons. In an attempt to enhance such possible effects, we have repeated our calculation of $\langle \bar{\zeta} \zeta \rangle$ for the pure gauge theory at and above the region

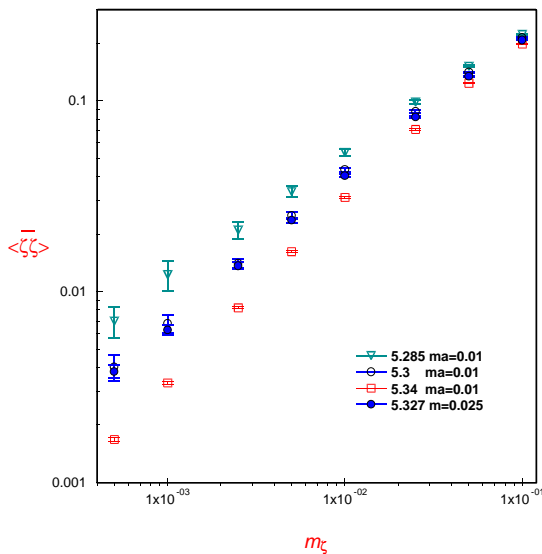


Figure 6. The quantity $\langle \bar{\zeta} \zeta \rangle$ plotted versus m_ζ for $\beta = 5.327$ and $ma = 0.025$. It is compared with $ma = 0.01$ results for three values of β . There is close agreement with the $ma = 0.01$, $\beta = 5.3$ curve.

of the deconfining phase transition. The results are summarized in Figure 7 where we plot the “quenched” chiral condensate, $\langle \bar{\zeta} \zeta \rangle$ as a function of β for a fixed mass value, $m_\zeta = 0.001$.

The results are quite surprising. Because of the lack of Z_3 symmetry for the Dirac operator, $\langle \bar{\zeta} \zeta \rangle$ shows dramatically different behavior in the three Z_3 phases for $\beta > \beta_c$. The two phases where the Wilson line has a complex expectation value (here called complex phases) show the same behavior for $\langle \bar{\zeta} \zeta \rangle$ because they are related by complex conjugation. This complex phase shows spontaneous breaking of chiral symmetry, with values of $\langle \bar{\zeta} \zeta \rangle$ that appear nearly continuous across the deconfinement phase transition. In contrast, the real phase has a vanishing value of $\langle \bar{\zeta} \zeta \rangle$ in the limit $m_\zeta \rightarrow 0$ and looks very much like the chirally symmetric phase seen in our full QCD simulations.

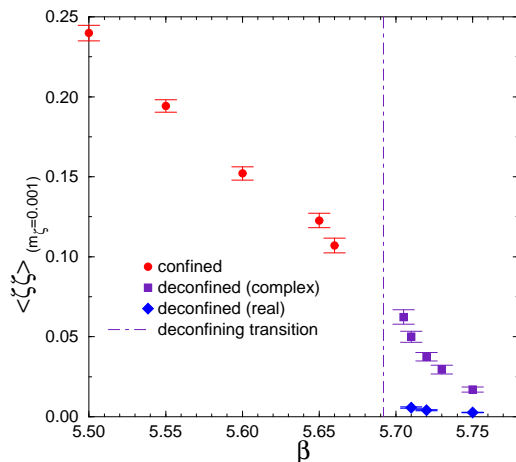


Figure 7. The quantity $\langle \bar{\zeta} \zeta \rangle$ evaluated at $m_\zeta = 0.001$ is shown as a function of β for pure $SU(3)$ gauge theory. The first-order, deconfining transition for $N_t = 4$ occurs at $\beta_c = 5.6925$. The multiple values for $\langle \bar{\zeta} \zeta \rangle$ shown for $\beta \geq \beta_c$ correspond to the real and complex phases with the smaller value of $\langle \bar{\zeta} \zeta \rangle$ occurring in the real phase.

4.1. Real phase

In Figure 8 we show $\langle \bar{\zeta} \zeta \rangle$ in the real phase as a function of quark mass, m_ζ . One sees a fractional power dependence $\langle \bar{\zeta} \zeta \rangle = 0.99(3) m_\zeta^{0.73(1)}$, very much like the behavior seen for $\beta > \beta_c$ in the full QCD simulations. As can be seen by comparing the results from the 16^3 and 32^3 volumes, this behavior appears to characterize the infinite volume limit.

Figure 9 compares the m_ζ dependence of $\langle \bar{\zeta} \zeta \rangle$ in this real phase with that of our full $N_f = 2$, $ma = 0.01$ simulations. The results are somewhat similar, showing perhaps a 15% variation. However, in contrast to the 0.01-0.025 comparison discussed earlier, there is a clear systematic difference between the quenched and full QCD results. As might be expected, the quenched results show an enhancement for small eigenvalues not seen in the $ma = 0.01$, two-flavor calculation. Nevertheless, we can describe the major effect of the fermion determinant on QCD thermodynamics as selecting the real phase (the phase with fewer small eigenvalues) as the physical phase.

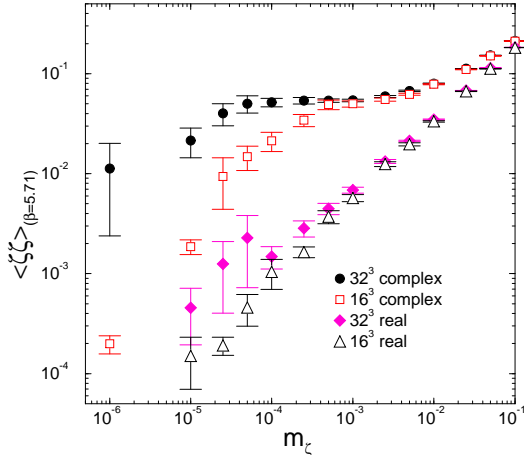


Figure 8. A comparison of $\langle \bar{\zeta}\zeta \rangle$ as a function of m_ζ in the real and complex phases for $\beta = 5.71$ and 16^3 and 32^3 volumes. The real phase shows no perceptible volume dependence while the complex phase changes significantly.

4.2. Complex phase

We see chiral symmetry breaking in the complex, deconfined phase as might be expected from a dilute instanton gas model. In Figure 8 we explicitly compare the dependence of $\langle \bar{\zeta}\zeta \rangle$ on quark mass for 16^3 and 32^3 volumes. As can be seen, the presumed finite-volume “knee”, where $\langle \bar{\zeta}\zeta \rangle$ abruptly begins to decrease with decreasing quark mass dramatically shifts to smaller quark mass on the larger volume. The shift by roughly the factor of 8 by which the volume has increased is exactly what is expected for such spontaneous symmetry breaking.

The variation of $\langle \bar{\zeta}\zeta \rangle$ with m_ζ is quite similar to that seen for $\beta < \beta_c$ in our two-flavor simulations. For smaller β a constant plus linear fit to $\langle \bar{\zeta}\zeta \rangle$ as a function of m_ζ works quite well but as β increases and the constant intercept decreases, a constant plus fraction power fit works significantly better. This effect is best seen on 32^3 volumes and in Figure 10 we show $\langle \bar{\zeta}\zeta \rangle$ versus m_ζ for a series of β values. This similarity with our $\beta < \beta_c$, $N_f = 2$ simulations suggests the possibility of a second, chiral symmetry restoring transition in $\langle \bar{\zeta}\zeta \rangle$ for this complex, deconfined phase. In Figure 11 we plot the $m_\zeta \rightarrow 0$ values from the constant plus

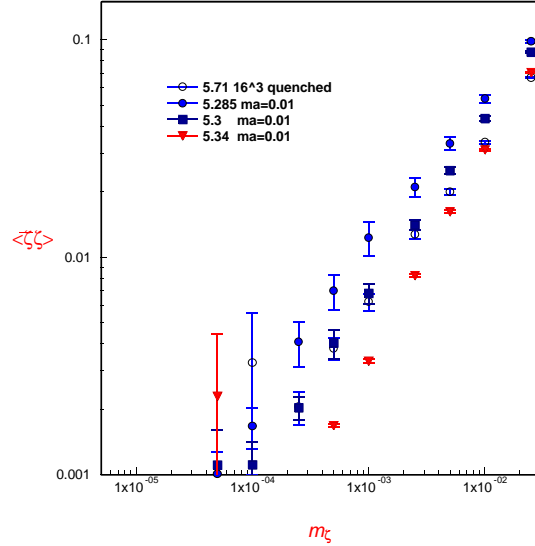


Figure 9. A comparison of $\langle \bar{\zeta}\zeta \rangle$ plotted as a function of m_ζ computed the real, quenched phase at $\beta = 5.71$ (open circles) with our $ma = 0.01$, two-flavor results for a series of values of β . Although the $\beta = 5.34$, full QCD results (solid inverted triangles) match most closely for larger quark masses, as m_ζ decreases, the full QCD chiral condensate falls more rapidly.

fractional power fits, versus β . Clearly we cannot rule out such a second phase transition although a continuous, rapid decrease in $\langle \bar{\zeta}\zeta \rangle|_{m_\zeta=0}$ as β increases above the first-order critical point appears the most natural interpretation of the data.

4.3. Inconsistent $N_f = 1$ Phase Transition

Combining our $N_f = 2$ results with this $N_f = 0$ calculation suggests that the one-flavor phase transition may be quite different from that expected on theoretical grounds, at least for correspondingly coarse lattice spacings. Since the density of small eigenvalues found in the “real” deconfined phase for pure QCD is insufficient to support a non-zero value of $\langle \bar{\zeta}\zeta \rangle$, the $N_f = 1$ high temperature phase, with increased suppres-

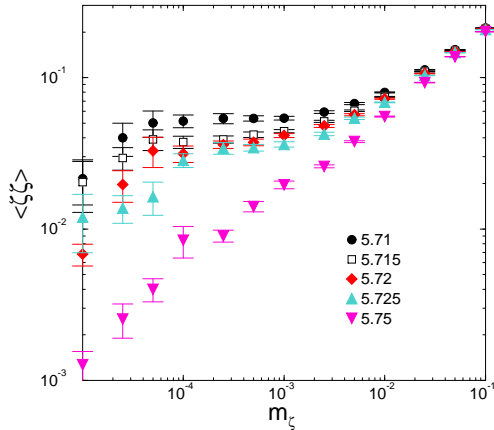


Figure 10. The quenched chiral condensate in the complex phase, plotted versus m_ζ using only 32^3 volumes for a series of values of $\beta > \beta_c$. The curves are well fit by a constant plus a fractional power for $m_\zeta > 10^{-4}$.

sion of small eigenvalues coming from the fermion determinant, should also show exact chiral symmetry with $\langle \bar{\chi}\chi \rangle = 0$ in the limit $m \rightarrow 0$. Thus, for $N_f = 1$, $\langle \bar{\chi}\chi \rangle_{m=0}$ is non-zero for strong coupling but may well vanish for weak coupling which would require that $N_f = 1$ will show a phase transition. This is in conflict with the usual analysis which concludes that there is no transition because of the anomalous breaking of the theory's $U(1)$ chiral symmetry.

The failure to see the behavior expected for $N_f = 1$ would be a serious cause of concern either about our understanding of continuum thermodynamics or about the coarse lattice spacings used in present-day lattice calculations.

5. CONCLUSION

It should be noted that we have adopted a new approach to the study of the axial anomaly using staggered fermions. Direct investigation of the axial anomaly is normally impeded by the absence of a conserved, flavor-singlet axial current defined on the lattice. For example, a quantity like the η' mass will receive contributions from both chirally-asymmetric lattice artifacts as well as the small Dirac eigenvalues of physical interest.

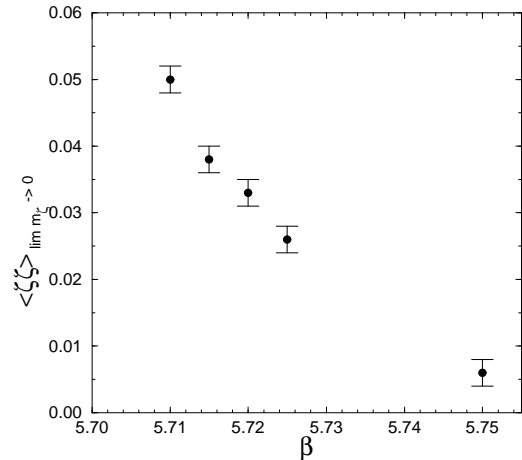


Figure 11. The constant term in our constant plus fractional power fit, plotted against β . We cannot distinguish with certainty between the presence of a second, chiral symmetry restoring transition for $\beta \approx 5.75$ and a rapid decrease of $\langle \bar{\zeta}\zeta \rangle |_{m_\zeta \rightarrow 0}$ as β rises, although the latter interpretation appears to be favored.

By using operators with a different number of flavors than appear in the Dirac determinant (operators which obey an exact chiral symmetry on the lattice), we can study directly the effects of the relevant Dirac spectrum—a quantity determined solely by the number of flavors in the fermion determinant. The zero-momentum two-point function ω of Eq. 7 examined for $N_f = 2$ and the four-flavor chiral condensate $\langle \bar{\zeta}\zeta \rangle$ discussed for $N_f = 1$ are examples of this strategy.

REFERENCES

1. T. Banks and A. Casher, Nucl. Phys. B169 (1980) 103.
2. R. D. Pisarski and F. Wilczek, Phys. Rev. D29 (1984) 338.
3. For a recent review of this topic see C. Detar, Nucl. Phys. B (proc. suppl.) 42 (1995) 73.